Bound free electron-positron pair production accompanied by giant dipole resonances

M. Y. Şengül[1,2] and M. C. Güçlü[1]
[1]*İstanbul Technical University, Faculty of Science and Letters, TR-34469 İstanbul, Turkey*
[2]*Kadir Has University, Faculty of Science and Letters, TR-34083 Cibali, Fatih-İstanbul, Turkey*
(Received 18 February 2010; revised manuscript received 24 September 2010; published 10 January 2011)

At the Relativistic Heavy Ion Collider (RHIC) and the Large Hadron Collider (LHC), for example, virtual photons produce many particles. At small impact parameters where the colliding nuclei make peripheral collisions, photon fluxes are very large and these are responsible for the multiple photonuclear interactions. Free pair productions, bound free pair productions, and nuclear Coulomb excitations are important examples of such interactions, and these processes play important roles in the beam luminosity at RHIC and LHC. Here we obtained the impact parameter dependence of bound free pair production cross sections and by using this probability we obtained bound free electron-positron pair production with nuclear breakup for heavy ion collisions at RHIC and LHC. We also compared our results to the other calculations.

DOI: 10.1103/PhysRevC.83.014902 PACS number(s): 25.75.Cj, 25.30.Rw, 24.30.Cz

I. INTRODUCTION

In the Relativistic Heavy Ion Collider (RHIC) for Au + Au collisions and in the Large Hadron Collider (LHC) for Pb + Pb collisions, the cross sections of the electromagnetic production of lepton pairs are very large because heavy ions that have a large charge (Z) produce strong electromagnetic fields. If one of the fully stripped ions captures one of the produced electrons, it depletes the beam and this limits the luminosity of the ion beam. There are several calculations about the bound free pair production [1–3] and the cross section behaves as

$$\sigma_{\mathrm{BFPP}} \propto Z_a^5 Z_b^2 \ln\left(\frac{\gamma}{\Delta}\right), \tag{1}$$

where Z_a and Z_b are the charge numbers of the ion capturing electrons, and Δ is a slowly varying parameter.

When the impact parameter b is smaller than twice the nuclear radius R, the hadronic interactions that are the main interests of the experiments occur. In ultraperipheral collisions $b > 2R$, where b is greater than twice the nuclear radius R. Photonuclear reactions and electromagnetic interactions can be detected in ultraperipheral collisions [4–8]. In ultrarelativistic heavy ion colliders, such as RHIC and LHC, there are two dominant processes that restrict the luminosity of the ion beams: bound free electron-positron pair production (BFPP) and giant dipole resonance (GDR). In both processes, each ion is acted on by the Lorentz contracted electromagnetic field of the other ion. In the BFPP, an electron is captured by one of the colliding ions and leads to the loss of the ion from the beam. This leads to a change in the charge of the ion and causes the ion to fall out of the beam. The importance of BFPP for beam losses and the quenching limit of the LHC was discussed in the literature [1,2,9–17]. In the GDR, the Coulomb force dissociates the nucleus where the protons and neutrons oscillate against each other. Then the neutrons fall out of the beam. Each of these processes causes the limitation of the beam lifetime for the collisions of Au + Au at RHIC or Pb + Pb at LHC [18,19].

Bruce *et al.* [4], accelerator physicists at LHC, restudied the question of Pb^{81}-induced magnet quenches, and they presented simulation results for the case of $^{208}Pb^{82+}$ ion operation in the LHC. They concluded that the expected heat load during nominal $^{208}Pb^{82+}$ operation is 40% above the quench level and this limits the maximum available luminosity. The only measurement of BFPP at RHIC used copper beams [9] and they looked at a single-electron atom. The calculated theoretical cross sections predict this measurement.

Recently, the STAR Collaboration measured electron-positron pairs [20] together with the electromagnetic excitation of both ions, predominantly to the giant dipole resonance. The STAR Collaboration used gold atoms at $\sqrt{s_{NN}} = 200$ GeV/nucleon energies. The decay of the excited nucleus generally emits one or two neutrons and these neutrons are detected in the forward zero degree calorimeter.

II. FORMALISM

In this work, we calculate the cross section of BFPP with the GDR of the ions in lowest-order QED as shown in Fig. 1. We use the semiclassical approximation in the calculation and the Monte Carlo method to obtain the exact results in Ref. [19]. In the bound free pair production accompanied by giant dipole resonance, the electron is captured by one of the colliding ions that is nuclear excited:

$$Z_a + Z_b \rightarrow (Z_a^* + e^-)_{1s_{1/2},\ldots} + Z_b^* + e^+, \tag{2}$$

which leads to the loss of the (one-electron) excited ion from the beam. In our calculations, Monte Carlo techniques were used, and the integrands were tested on about 10 million randomly chosen "positions" to ensure sufficient convergence of our theoretical results. The total numerical error in the computations is estimated to be less than or approximately 5%. And then we calculate the impact parameter dependence cross section of BFPP accompanied by GDR, and by using this result we calculate the transverse momentum, longitudinal momentum, energy, and rapidity distribution of the produced positrons.

After the electron-positron pairs are created, the electron is captured by one of the colliding ions and then the positron becomes free, which is described by the plane waves

$$\Psi_q^{(+)} = N_+\left[e^{i\mathbf{q}\cdot\mathbf{r}}\mathbf{u}_{\sigma_q}^{(+)} + \Psi'\right], \tag{3}$$

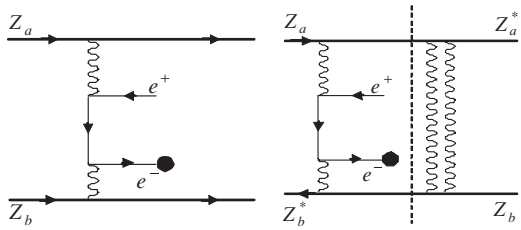

FIG. 1. Dominant Feynman diagrams for two photon reactions: (a) BFPP and (b) BFPP accompanied by GDR in a relativistic heavy ion collision. We assume that BFPP (left of the dashed line) is independent of the nuclear excitation (right of the dashed line).

and together with the (correction) term Ψ' and this is the distortion due to the charge of one of the nuclei. In expression (3), moreover,

$$N_+ = e^{-\pi a_+/2}\Gamma(1+ia_+), \quad a_+ = \frac{Ze^2}{v_+}, \tag{4}$$

is a normalization constant that accounts for the distortion of the wave function that is acceptable for $Z\alpha \ll 1$ [13,16,21], and where $\alpha = e^2/\hbar c \cong 1/137$ is the fine structure constant and v_+ is the velocity of the positron in the rest frame of the ion, into which the electron is captured in the course of process (2).

For the outgoing positron, the spinor structure is

$$\mathbf{u}_{\sigma_q}^{(+)} = \sqrt{\frac{E_q^{(+)}+mc^2}{2mc^2}}\begin{bmatrix}\phi^{(s)}\\ \frac{\boldsymbol{\sigma}\cdot\mathbf{p}c}{E_q^{(+)}+mc^2}\phi^{(s)}\end{bmatrix} \tag{5}$$

(for spinors with positive energy $E_q^{(+)} > 0$), where $\phi^{(s)} = \chi_{1/2}^{(s)}$ denotes a Pauli spinor and $s = \pm 1/2$ its spin projection.

After the pair production has occurred, the electron is captured by one of the ions and, thus, needs to be described as a bound state. In a semirelativistic approximation, these electron states are often represented by [22,23]

$$\Psi^{(-)} = \left(1 - \frac{i}{2m}\boldsymbol{\alpha}\cdot\boldsymbol{\nabla}\right)\mathbf{u}\Psi_{\text{nonrel}}(r), \tag{6}$$

that is, in terms of the nonrelativistic (ground) state function

$$\Psi_{\text{nonrel}}(r) = \frac{1}{\sqrt{\pi}}\left(\frac{Z}{a_H}\right)^{3/2} e^{-Zr/a_{\text{H}}} \tag{7}$$

of the hydrogenlike ion, where $\mathbf{u}$ represents the spinor part of the captured electron and $a_{\text{H}} = 1/e^2$ is the Bohr radius of atomic hydrogen.

Using the positron (Sommerfeld-Maue wave function) and the captured electron (Darwin wave function) states from above, the direct Feynman diagram for the second-order perturbation calculation can be written as

$$\begin{aligned}\langle\Psi^{(-)}|S_{ab}|\Psi_q^{(+)}\rangle &= i\sum_p\sum_s\int_{-\infty}^{\infty}\frac{d\omega}{2\pi}\frac{\langle\Psi^{(-)}|V_a(\omega-E^{(-)})\big|\chi_p^{(s)}\big\rangle\big\langle\chi_p^{(s)}\big|V_b(E_q^{(+)}-\omega)|\Psi_q^{(+)}\rangle}{\left(E_p^{(s)}-\omega\right)}\\ &= i\sum_p\sum_s\int_{-\infty}^{\infty}\frac{d\omega}{2\pi}\int_{-\infty}^{\infty}d^3\mathbf{r}\left(1+\frac{i}{2m}\boldsymbol{\alpha}\cdot\boldsymbol{\nabla}\right)\Psi_{\text{nonrel}}(r)e^{i\mathbf{p}\cdot\mathbf{r}}A_a(\mathbf{r};\omega-E^{(-)})\\ &\quad\times\int_{-\infty}^{\infty}d^3\mathbf{r}'N_+e^{-i(\mathbf{p}-\mathbf{q})\cdot\mathbf{r}'}A_b(\mathbf{r}';E_q^{(+)}-\omega)\frac{\langle\mathbf{u}|(\mathbf{1}-\beta\alpha_{\mathbf{z}})\big|\mathbf{u}_{\sigma_{\mathbf{p}}}^{(\mathbf{s})}\big\rangle\big\langle\mathbf{u}_{\sigma_{\mathbf{p}}}^{(\mathbf{s})}\big|(\mathbf{1}+\beta\alpha_{\mathbf{z}})\big|\mathbf{u}_{\sigma_{\mathbf{q}}}^{(+)}\big\rangle}{\left(E_p^{(s)}-\omega\right)},\end{aligned} \tag{8}$$

where V_a and V_b are the potentials of nuclei a and b.

The transition matrix element for a fixed spin and momentum state of the positron as well as for a given intermediate state can be expressed as

$$\begin{aligned}\langle\Psi^{(-)}|S_{ab}|\Psi_q^{(+)}\rangle = \frac{iN_+}{2\beta}\frac{1}{\sqrt{\pi}}\left(\frac{Z}{a_{\text{H}}}\right)^{3/2}\int\frac{d^2p_\perp}{(2\pi)^2}e^{i(\mathbf{p}_\perp-\frac{\mathbf{q}_\perp}{2})\cdot\mathbf{b}}\\ \times F(-\mathbf{p}_\perp:\omega_a)F(\mathbf{p}_\perp-\mathbf{q}_\perp:\omega_b)\\ \times\mathcal{T}_q(\mathbf{p}_\perp:+\beta),\end{aligned} \tag{9}$$

where $\mathbf{b}$ is the impact parameter of the ion-ion collision, and the function $F(q,\omega)$ can be described as the scalar part of the field associated with ions a and b in momentum space. The explicit form of these scalar fields can be written in terms of the corresponding frequencies as

$$F(-\mathbf{p}_\perp:\omega_a) = \frac{4\pi Ze}{\left(\frac{Z^2}{a_{\text{H}}^2}+\frac{\omega_a^2}{\gamma^2\beta^2}+\mathbf{p}_\perp^2\right)} \tag{10a}$$

for the frequency ω_a, and as

$$F(\mathbf{p}_\perp-\mathbf{q}_\perp:\omega_b) = \frac{4\pi Ze\gamma^2\beta^2}{\left[\omega_b^2+\gamma^2\beta^2(\mathbf{p}_\perp-\mathbf{q}_\perp)^2\right]} \tag{10b}$$

for the frequency ω_b, respectively. Apart from the scalar field of each ion, Eq. (9) also contains the transition amplitudes $\mathcal{T}$, which relate the intermediate photon lines to the outgoing electron-positron lines. This amplitude depends explicitly on the (relative) velocity of the ions (β), the transverse momentum ($\mathbf{p}_\perp$), and the momentum of the positron (q), and it is given by

$$\begin{aligned}\mathcal{T}_q(\mathbf{p}_\perp:+\beta) = \sum_s\sum_{\sigma_p}\frac{1}{\left[E_p^{(s)}-\left(\frac{E^{(-)}+E_q^{(+)}}{2}\right)-\beta\frac{q_z}{2}\right]}\\ \times\left[1+\frac{\boldsymbol{\alpha}\cdot\mathbf{p}}{2m}\right]\langle\mathbf{u}|(\mathbf{1}-\beta\alpha_{\mathbf{z}})\big|\mathbf{u}_{\sigma_{\mathbf{p}}}^{(\mathbf{s})}\big\rangle\\ \times\big\langle\mathbf{u}_{\sigma_{\mathbf{p}}}^{(\mathbf{s})}\big|(\mathbf{1}+\beta\alpha_{\mathbf{z}})\big|\mathbf{u}_{\sigma_{\mathbf{q}}}^{(+)}\big\rangle.\end{aligned} \tag{11}$$

In this amplitude, the parallel component of the intermediate-state momentum is described by p_z. The integration over the impact parameter b in Eq. (9) can also be carried out analytically. Following similar lines as in a direct diagram, the crossed-term amplitude $\langle\Psi^{(-)}|S_{ba}|\Psi_q^{(+)}\rangle$ can be evaluated.

Having the amplitudes for the direct S_{ab} and crossed S_{ba} diagram, the cross section for the generation of a bound free electron-positron pair in collisions of two heavy ions can be written as

$$\sigma_{\mathrm{BFPP}} = \int d^2b \sum_{q<0} \left|\langle\Psi^{(-)}|S\left|\Psi_q^{(+)}\right\rangle\right|^2, \tag{12}$$

where $S = S_{ab} + S_{ba}$ denotes the sum of the direct and crossed terms. After all the simplifications from above, these cross sections for the BFPP can be expressed as

$$\begin{aligned}\sigma_{\mathrm{BFPP}} &= \int d^2b \sum_{q<0} \left|\langle\Psi^{(-)}|S_{ab}\left|\Psi_q^{(+)}\right\rangle + \langle\Psi^{(-)}|S_{ba}\left|\Psi_q^{(+)}\right\rangle\right|^2 \\ &= \frac{|N_+|^2}{4\beta^2}\frac{1}{\pi}\left(\frac{Z}{a_{\mathrm{H}}}\right)^3 \sum_{\sigma_q}\int \frac{d^3q d^2p_\perp}{(2\pi)^5}[\mathcal{A}^{(+)}(q:\mathbf{p}_\perp) \\ &\quad + \mathcal{A}^{(-)}(q:\mathbf{q}_\perp - \mathbf{p}_\perp)]^2, \end{aligned} \tag{13}$$

where

$$\mathcal{A}^{(+)}(q:\mathbf{p}_\perp) = F(-\mathbf{p}_\perp:\omega_a)F(\mathbf{p}_\perp - \mathbf{q}_\perp:\omega_b)\mathcal{T}_q(\mathbf{p}_\perp:+\beta) \tag{14a}$$

and

$$\begin{aligned}\mathcal{A}^{(-)}(q:\mathbf{q}_\perp - \mathbf{p}_\perp) &= F(\mathbf{p}_\perp - \mathbf{q}_\perp:\omega_b)F(-\mathbf{p}_\perp:\omega_a) \\ &\quad \times \mathcal{T}_q(\mathbf{q}_\perp - \mathbf{p}_\perp:-\beta)\end{aligned} \tag{14b}$$

are some proper products of the transition amplitudes and scalar parts of the fields as associated with ions a and b. All these functions were displayed explicitly in Eqs. (1) and (11) [19].

We found an expression for the impact parameter dependence cross section of free-pair production in Ref. [24]. We used the same method to calculate the impact parameter dependence BFPP cross section. Because it contains a highly oscillatory Bessel function of order zero, we divide the integration according to

$$\frac{d\sigma_{\mathrm{BFPP}}}{db} = \int_0^\infty dq q b J_0(qb)\mathcal{F}(q), \tag{15}$$

where $\mathcal{F}(q)$ is a six-dimensional integral. In the above equation, the function $J_0(qb)$ is a rapidly oscillating function, particularly for large b, making it impossible to apply the Monte Carlo techniques. However, for a fixed value of positron momentum q, the Monte Carlo technique can be generalized to calculate the six-dimensional above integral $\mathcal{F}(q)$:

$$\begin{aligned}\mathcal{F}(q) &= \frac{\pi}{8\beta^2}|N_+|^2\frac{1}{\pi}\left(\frac{Z}{a_{\mathrm{H}}}\right)^3 \sum_{\sigma_q}\int_0^{2\pi} d\phi_q \int \frac{dq_z d^2K d^2Q}{(2\pi)^7} \\ &\quad \times \left\{F\left[\frac{1}{2}(\mathbf{Q}-\mathbf{q});\omega_a\right]F[-\mathbf{K};\omega_b]\mathcal{T}_q\left[-\frac{1}{2}(\mathbf{Q}-\mathbf{q});\beta\right]\right. \\ &\quad \left. + F[-\mathbf{K};\omega_b]F\left[\frac{1}{2}(\mathbf{Q}-\mathbf{q});\omega_a\right]\mathcal{T}_q[\mathbf{K};-\beta]\right\} \\ &\quad \times \left\{F\left[\frac{1}{2}(\mathbf{Q}+\mathbf{q});\omega_a\right]F[-\mathbf{K};\omega_b]\mathcal{T}_q\left[-\frac{1}{2}(\mathbf{Q}+\mathbf{q});\beta\right]\right. \\ &\quad \left. + F[-\mathbf{K};\omega_b]F\left[\frac{1}{2}(\mathbf{Q}+\mathbf{q});\omega_a\right]\mathcal{T}_q[\mathbf{K};-\beta]\right\}. \end{aligned} \tag{16}$$

In Eq. (16), N_+ is the normalization constant that comes from the positron wave function; the Z/a_{H} term comes from the electron wave function. Here $\mathbf{q}$ is the momentum of the positron, and $\mathbf{Q}$ and $\mathbf{K}$ are the new variables that are the functions of $\mathbf{q}_\perp$ and $\mathbf{p}_\perp$. We performed a similar calculation for the free electron-positron pair production in Ref. [24], and all the functions and parameters in Eq. (16) are explained in detail there. We should note that integral variables for the bound free case obtained in Ref. [24] are six in contrast to the free-pair production, which has nine variables. When we integrate Eq. (16) numerically over all variables for fixed values of q, we obtain the very simple function $\mathcal{F}(q)$:

$$\mathcal{F}(q) = \mathcal{F}(0)e^{-aq} = \sigma_{\mathrm{BFPP}}e^{-aq}, \tag{17}$$

where $\mathcal{F}(0)$ is the value of the function at $q = 0$ and it is the total cross section σ_{BFPP} which is equal to Eq. (1). In Eq. (17), a is the slope of the function $\mathcal{F}(q)$ and it is a constant that is independent of the charges and energies of the heavy ions as seen in Fig. 2. The function $\mathcal{F}(q)/\mathcal{F}(0)$ is obtained for the charges of heavy ions in the range $Z_{a,b} = 20$–90 and for the energies in the range $\gamma = 10$–3400. In this figure, each point is calculated with the Monte Carlo method to about 5% error. From this calculation, we can approximately write the slope $a = 1.35\lambda_C$.

Finally, by using Eq. (15), we can write the impact parameter dependence cross section as

$$\frac{d\sigma_{\mathrm{BFPP}}}{db} = \sigma_{\mathrm{BFPP}}\frac{a\,b}{(a^2+b^2)^{3/2}}. \tag{18}$$

Figure 3 shows differential cross sections of the transverse momentum of the produced positrons for free and bound free cases. From this figure, it becomes clear that the bound free and free-pair production distributions display a rather similar behavior. More information can be found in Ref. [19]. At the end of our calculations, we can write the impact parameter

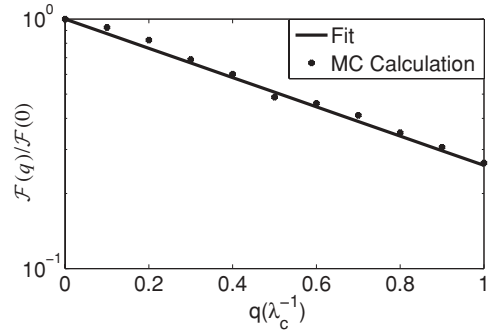

FIG. 2. The function $\mathcal{F}(q)/\mathcal{F}(0)$ is calculated for the charges of heavy ions in the range $Z_{a,b} = 20$–90 and for the energies in the range $\gamma = 10$–3400. The points show the results of the Monte Carlo calculations for each q value and the smooth curve is our fit for these points. The slope of this function gives the value of a as $1.35\lambda_c$.

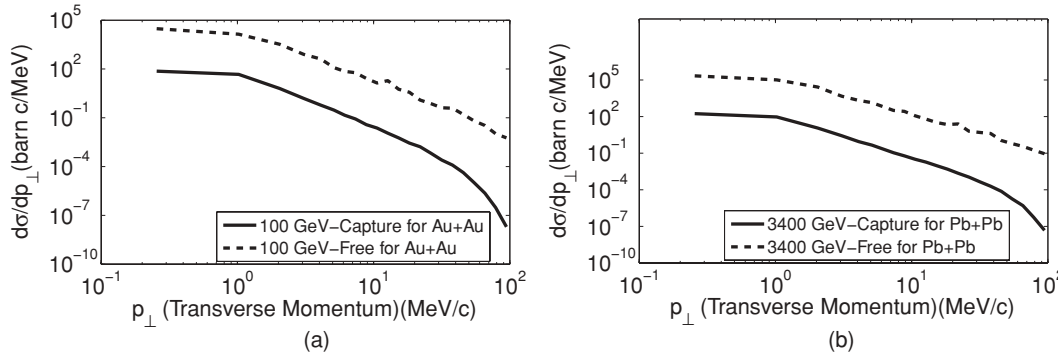

FIG. 3. Differential cross section as a function of the transverse momentum ($p_\perp$) of the produced positrons. Calculated differential cross sections are shown for the two collision systems (a) Au + Au at RHIC-100 GeV/nucleon and (b) Pb + Pb at LHC-3400 GeV/nucleon, respectively. When compared with the production of free electron-positron pairs, the BFPP cross section for the capture of the electron into the $1s$ ground state is suppressed by about three orders of magnitude for all transverse momenta between 0.1 and 100 MeV/c [19].

dependence probability for bound free pair production as

$$P(b) = \sigma_{\mathrm{BFPP}} \frac{a}{2\pi(a^2+b^2)^{3/2}}. \tag{19}$$

In our previous work, we wrote the impact parameter dependence probability for free pair production as [24]

$$P(b) = \sigma_{\mathrm{free}} \frac{a}{2\pi(a^2+b^2)^{3/2}}. \tag{20}$$

III. RESULTS AND DISCUSSIONS

Recent papers [20,25–27] reported on the electromagnetic production of free electron-positron pairs accompanied by GDR at the RHIC for Au + Au collisions. In this article, we calculate bound free electron-positron pair production accompanied by GDR, and this process can be seen in Fig. 1. In addition to the lepton pairs, the nuclei also exchange some photons and this may break up the nuclei. After the GDR, if the nucleus emits only one neutron we show this as $(1n)$ and it is the subset of (Xn). And in (Xn), a general Coulomb excitation leads to the emission of any number of neutrons [18,28].

For the probability of GDR excitation in one ion, we use the approximation

$$P_{C(1n)}(b) = P^1_{C(1n)}(b) e^{-P^1_C(b)}, \tag{21}$$

where

$$P^1_C(b) = S/b^2 \tag{22}$$

with

$$S = \frac{2\alpha^2 Z^3 N}{A m_N \omega} \approx 5.45 \times 10^{-5} Z^3 N A^{-2/3} \mathrm{fm}^2, \tag{23}$$

where m_N is the nucleon mass and the neutron, proton, and mass numbers of the ions are N, Z, and A, respectively. The excitation probability is inversely proportional to the energy $\omega \approx 80$ MeV $A^{-1/3}$ of the GDR state [29]. At small impact parameters, $P^1_C(b)$ can exceed 1; then this cannot be interpreted as a probability. Instead, it corresponds to the mean number of excitations. In more detail, $P^1_{C(Xn)}(b)$ is the mean number of excitations; the probability of having exactly N excitations follows a Poisson distribution. The probability for at least one Coulomb excitation is

$$P_{C(Xn)}(b) = 1 - e^{(-P^1_{C(Xn)}(b))}. \tag{24}$$

In mutual Coulomb dissociation (MCD), the two nuclear breakups occur independently, so the probability for MCD is [18,28]

$$P_{C(XnXn)}(b) = [P_{C(Xn)}(b)]^2 \tag{25}$$

and

$$P_{C(1n1n)}(b) = [P_{C(1n)}(b)]^2. \tag{26}$$

The excitation probability may be determined by a unitarization procedure.

The total cross section for BFPP with mutual nuclear excitation is

$$\sigma^{\mathrm{GDR}}_{\mathrm{BFPP}} = 2\pi \int_{b_{\min}}^{\infty} dbb P_{\mathrm{BFPP}}(b) P^2_{C(1n)}(b) P_{\text{no had}}(b) \tag{27}$$

where $P_{\mathrm{BFPP}}(b)$ is the probability of BFPP, $P_{C(1n)}(b)$ is the probability of simultaneous nuclear excitation as a function of impact parameter, and $P_{\text{no had}}(b)$ is the probability of no hadronic interaction happening between the nuclei. No hadronic interaction probability is calculated in the usual Glauber manner from impact-parameter-dependent nuclear density overlap. The nuclear charge density is assumed to have a Woods-Saxon distribution [27,30].

TABLE I. Integrated cross sections for Au + Au collisions at RHIC energies and for Pb + Pb collisions at LHC energies for free pair production and bound free pair production. Our work is compared with the calculations of Baltz for RHIC energies.

	Untagged $\sigma(b)$	$1n1n$ $\sigma_{\mathrm{tagged}}(mb)$	$XnXn$ $\sigma_{\mathrm{tagged}}(mb)$
Au + Au at RHIC-Free	3.40×10^4	1.63×10^3	1.98×10^3
Pb + Pb at LHC-Free	2.12×10^5	10.2×10^3	12.4×10^3
Au + Au at RHIC-BFPP	94.5	4.5	5.5
Au + Au at RHIC-Baltz-BFPP	88.8	1.1	1.4
Pb + Pb at LHC-BFPP	202	9.7	11.7

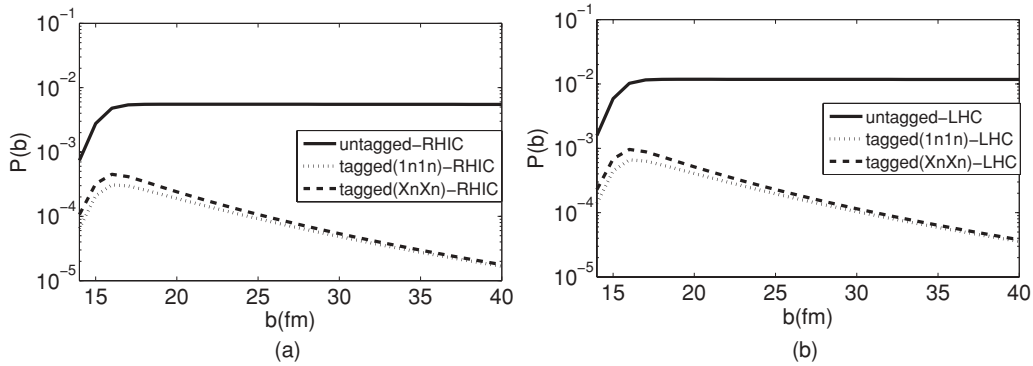

FIG. 4. Probability of positron production with (a) gold beams at RHIC and (b) lead beams at the LHC as a function of b with $XnXn$ (dashed line) and $1n1n$ (dotted line) and without nuclear excitation (solid line).

Baltz and his co-workers [31] calculated the cross section for the bound free pair production by using Coulomb-Dirac wave functions in a formulation which exhibits naturally the same impact parameter cutoff as the Weizsacker-Williams method. And their approximated cross section for the bound free pair production at RHIC energies for Au + Au collisions is equal to

$$\sigma_{\mathrm{BFPP}} = 11.2 \ln \gamma - 24(\mathrm{b}). \tag{28}$$

Baltz and his co-workers [32] approximately determined the cross section for the bound free pair production at RHIC energies for Pb + Pb collisions:

$$\sigma_{\mathrm{BFPP}} = 14.3 ln\gamma - 31\ (\mathrm{b}). \tag{29}$$

To obtain the total bound free pair production cross sections for different colliding ions, the charge dependence is approximately as $Z^{6.7}$, at least for ion pairs that range from iodine to uranium [32]. By using these approximations for the bound free pair production, the cross section for RHIC energies in Au + Au collisions is equal to 88.8 b and the cross section for RHIC energies in Pb + Pb collisions is equal to 113 b. In Ref. [33], Baltz numerically calculated the probabilities for each of the listed impact parameters using Coulomb-Dirac wave functions for the bound electron and the continuum positrons. By calculating those numerical results, the scheme was laid out in a series of papers [1,31,34,35]. In this article, we aimed to compare our impact-parameter-dependent probability function with the results of Baltz. For this, by using the data given in Ref. [33] for Pb + Pb collisions at RHIC energies, we fitted a function that appropriates them which can be written as

$$P(b) = \frac{228.807}{(1.72134 \times 10^{10} + b^4)^{1/2}}. \tag{30}$$

TABLE II. Integrated cross sections for Pb + Pb collisions at RHIC energies by using our calculations and for the same collision at RHIC energies by using the calculations of Baltz.

	Untagged $\sigma_{\mathrm{BFPP}}(b)$	$1n1n$ $\sigma_{\mathrm{tagged}}(mb)$	$XnXn$ $\sigma_{\mathrm{tagged}}(mb)$
Pb + Pb at RHIC	123	5.92	7.18
Pb + Pb at RHIC-Baltz	113	1.44	1.74

For Au + Au collisions at RHIC energies, the fitting function can be written as

$$P(b) = \frac{178.246}{(1.72134 \times 10^{10} + b^4)^{1/2}}. \tag{31}$$

Although this function is a simple and well-behaved function, integrating it over the impact parameter does not give a converged value for the total cross section. Therefore, they used a cutoff parameter γ/ω for the upper impact parameters, where γ is the Lorentz factor and ω is the energy difference. This cutoff parameter is the result of the Weizsacker-Williams method. However, in our method, there is no need to calculate an upper impact parameter and we take the integral limits from zero to infinity.

In Table I, some values of tagged and untagged cross sections are calculated for RHIC and LHC energies for free pair production and bound free pair production. We also compared our results with the calculations of Baltz at RHIC energies for bound free pair production. We calculated untagged bound free pair production cross sections and the results are 94.5 b for RHIC and 202 b for LHC collisions. Here we did not include the nuclear excitation processes and these values are shown in the first column in the table. When we include the nuclear excitation processes (mainly the GDR), the results are more than two orders of magnitude smaller than the untagged calculations.

In Table II, we compared our calculations with the work of Baltz for RHIC energies at Pb + Pb collisions. In Table III, we tabulated the BFPP cross sections with GDR (tagged) for minimum impact parameters of 14, 15, and 16 fm. Tagged cross sections for LHC collisions are about two times greater than RHIC collisions for various minimum impact parameters. In Fig. 4 we obtained the probability of positron production

TABLE III. Integrated cross sections for Au + Au collisions at RHIC energies and for Pb + Pb collisions at LHC energies for different impact parameters.

b_{min}	14 fm	15 fm	16 fm
$\sigma^{\mathrm{GDR}}_{\mathrm{BFPP}}$ (RHIC)	4.9 mb	4.5 mb	4.2 mb
$\sigma^{\mathrm{GDR}}_{\mathrm{BFPP}}$ (LHC)	10.6 mb	9.7 mb	8.9 mb

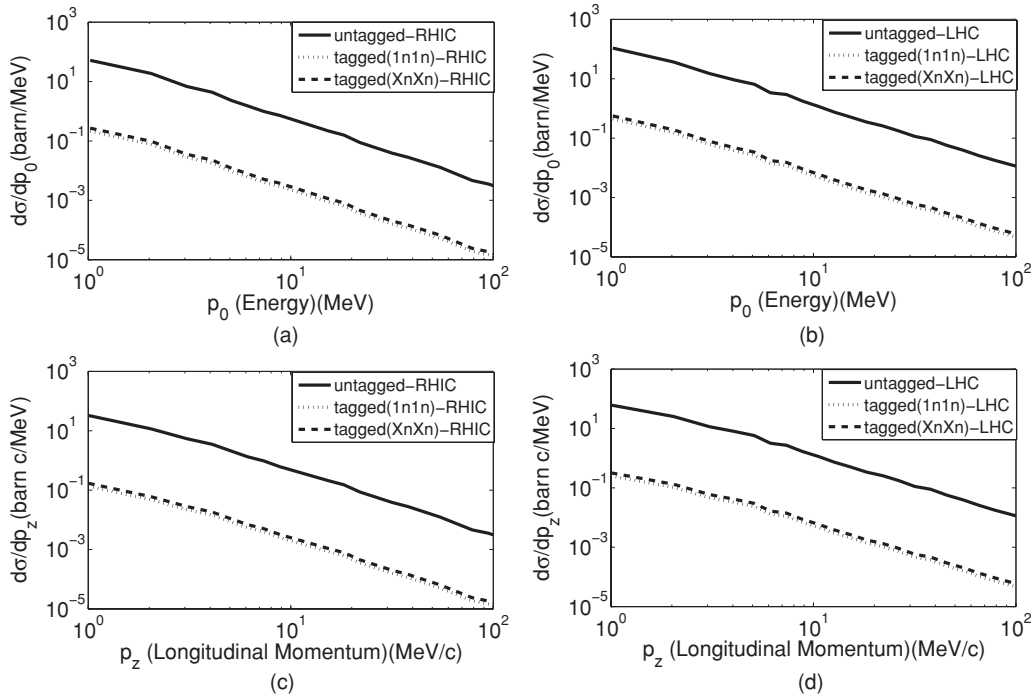

FIG. 5. Differential cross section as a function of the energy (p_0) of the produced positrons for (a) RHIC and (b) LHC; and as function of the longitudinal momentum (p_z) of the produced positrons for (c) RHIC and (d) LHC. The solid line is the total production, the dashed line is for $XnXn$, and the dotted line is $1n1n$.

with gold beams at RHIC and lead beams at the LHC as a function of impact parameter b. The solid line indicates the BFPP without nuclear excitation (untagged), the dashed line is the BFPP with $XnXn$ excitation, and the dotted line is BFPP with $1n1n$ excitation (tagged). In Fig. 5 we plot the differential cross section as a function of the energy (p_0) and longitudinal momentum (p_z) of the produced positrons for RHIC and LHC. The calculations show that both are the same

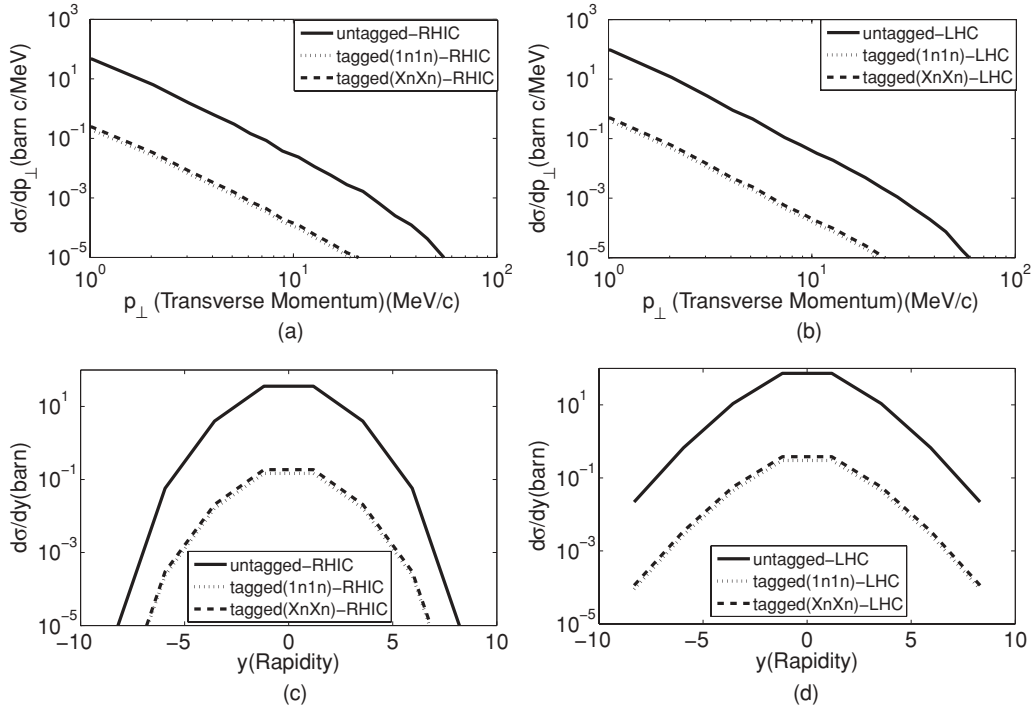

FIG. 6. Differential cross section as function of the transverse momentum ($p_\perp$) of the produced positrons for (a) RHIC and (b) LHC, and the differential cross section as a function of the rapidity (y) for (c) RHIC and (d) LHC. The solid line is the total production, the dashed line is for $XnXn$, and the dotted line is $1n1n$.

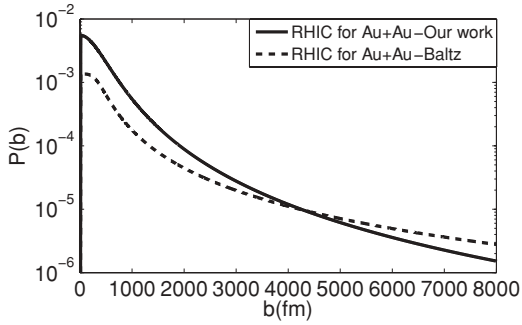

FIG. 7. Probability of positron production with gold beams at RHIC as a function of b; the solid line shows our work and the dashed line shows the work of Baltz.

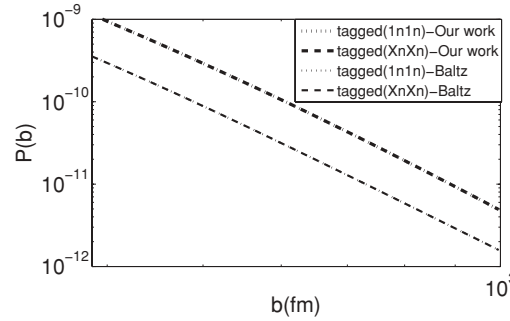

FIG. 8. Probability of positron production with gold beams at RHIC as a function of b for tagged($1n1n$) and tagged($XnXn$) results for our work and for the work of Baltz.

order of magnitude. In Fig. 6 we show the differential cross section as a function of the transverse momentum ($p_\perp$) of the produced positrons for RHIC and LHC. The transverse momentum distributions are consistently lower than energy and longitudinal momentum. In addition, we also calculated the differential cross section as a function of the rapidity (y) for RHIC and LHC.

In Fig. 7 we plot the impact parameter dependence probability function by using our approximated function and by using the function that we fitted with the help of the data given by Baltz [33]. We compared our probability function with the fitting probability function for the data of Baltz. The difference is that the fitting function goes to zero more slowly than our function because, for large impact parameters, it behaves like $\sim 1/b^2$ and our probability function for large impact parameters behaves as $\sim 1/b^3$.

In Fig. 8 we compare our results to the fitting function by using the data of Baltz for tagged($1n1n$) and tagged($XnXn$) states for the RHIC energies at Au + Au collisions. This plot shows that our calculations are about four times higher than the calculations of Baltz. In both calculations, as seen in the figure, the results of $1n1n$ and $XnXn$ are very close to each other.

IV. CONCLUSIONS

In this work, we obtained the impact-parameter-dependent cross section of bound free electron-positron pair production. By using this result, we calculated BFPP with GDR cross sections for $1n1n$ and $XnXn$ excitations. We also compared our results to the work of Baltz; our results are about four times larger. The main reason for this difference is the behavior of the impact-parameter-dependent probability of BFPP.

BFPP accompanied by GDR is an important electromagnetic interaction in relativistic heavy ion collisions. Although there is no way to directly measure the impact parameter experimentally, it is possible to select events with different impact parameter distributions. In this work, we obtained the impact-parameter-dependent BFPP which itself has a certain impact parameter distribution. BFPP accompanied by GDR excitation also has another impact parameter distribution. The combined reaction occurs mainly at small impact parameters. In STAR, the presence of mutual Coulomb excitation is used to select different impact parameter distributions to measure things like interference in ρ photoproduction [28,36]. The technique is applied to two-photon interactions by Baltz *et al.* [18]. There is a more analytical treatment by Baur *et al.* [26]. BFPP with Coulomb excitation presents an interesting complication, because the nucleus may be altered at the same time as the electron is captured. If the nuclear breakup includes proton (or higher charge) emission, then things might get complicated. This should not be a problem for GDR excitation of lead, because all of the relevant isotopes are stable, but it could be important for higher excitations, leading to multiple-particle emission.

ACKNOWLEDGMENTS

This research is partially supported by the Istanbul Technical University and Kadir Has University. We personally thank S. R. Klein and A. J. Baltz for valuable advice in calculating the cross sections and for the careful reading of our article.

[1] A. J. Baltz, M. J. Rhoades-Brown, and J. Weneser, Phys. Rev. A **50**, 4842 (1994).
[2] M. J. Rhoades-Brown, C. Bottcher, and M. R. Strayer, Phys. Rev. A **40**, 2831 (1989).
[3] H. Meier, Z. Halabuka, K. Hencken, D. Trautmann, and G. Baur, Phys. Rev. A **63**, 032713 (2001).
[4] R. Bruce, D. Bocian, S. Gilardoni, and J. M. Jowett, Phys. Rev. Spec. Top. **12**, 071002 (2009).
[5] M. C. Güçlü, Prog. Part. Nucl. Phys. **62**, 498 (2009).
[6] K. Hencken, D. Trautmann, and G. Baur, Phys. Rev. C **53**, 2532 (1996).
[7] K. Hencken, D. Trautmann, and G. Baur, Phys. Rev. C **59**, 841 (1999).
[8] A. J. Baltz, Phys. Rev. C **74**, 054903 (2006).
[9] R. Bruce, J. M. Jowett, S. Gilardoni, A. Drees, W. Fischer, S. Tepikian, and S. R. Klein, Phys. Rev. Lett. **99**, 144801 (2007).
[10] S. R. Klein, Nucl. Instrum. Methods A **459**, 51 (2001).

[11] A. Belkacem, H. Gould, B. Feinberg, R. Bossingham, and W. E. Meyerhof, Phys. Rev. Lett. **71**, 1514 (1993).
[12] H. F. Krause, C. R. Vane, S. Datz, P. Grafström, H. Knudsen, C. Scheidenberger, and R. H. Schuch, Phys. Rev. Lett. **80**, 1190 (1998).
[13] C. A. Bertulani and G. Baur, Phys. Rep. **163**, 299 (1988).
[14] A. J. Baltz *et al.*, Phys. Rep. **458**, 1 (2008).
[15] A. Aste, K. Hencken, D. Trautmann, and G. Baur, Phys. Rev. A **50**, 3980 (1994).
[16] C. A. Bertulani and D. Dolci, Nucl. Phys. A **683**, 635 (2001).
[17] G. Baur, K. Hencken, and D. Trautmann, Phys. Rep. **453**, 1 (2007).
[18] A. J. Baltz, Y. Gorbunov, S. R. Klein, and J. Nystrand, Phys. Rev. C **80**, 044902 (2009).
[19] M. Y. Şengül, M. C. Güçlü, and S. Fritzsche, Phys. Rev. A **80**, 042711 (2009).
[20] J. Adams *et al.*, Phys. Rev. C **70**, 031902(R) (2004).
[21] A. Aste, Europhys. Lett. **81**, 61001 (2008).
[22] V. B. Berestetskii, E. M. Lifshitz, and L. P. Pitaevskii, *Relativistic Quantum Field Theory* (Pergamon, New York, 1979).
[23] J. Eichler and W. E. Meyerhof, *Relativistic Atomic Collisions* (Academic, San Diego, CA, 1995).
[24] M. C. Güçlü, Nucl. Phys. A **668**, 149 (2000).
[25] C. A. Bertulani, S. R. Klein, and J. Nystrand, Annu. Rev. Nucl. Part. Sci. **55**, 271 (2005).
[26] G. Baur, K. Hencken, A. Aste, D. Trautmann, and S. R. Klein, Nucl. Phys. A **729**, 787 (2003).
[27] S. R. Klein and J. Nystrand, Phys. Rev. C **60**, 014903 (1999).
[28] A. J. Baltz, S. R. Klein, and J. Nystrand, Phys. Rev. Lett. **89**, 012301 (2002).
[29] K. Hencken, G. Baur, and D. Trautmann, Phys. Rev. C **69**, 054902 (2004).
[30] S. R. Klein, arXiv:nucl-ex/0310020.
[31] A. J. Baltz, M. J. Rhoades-Brown, and J. Weneser, Phys. Rev. A **48**, 2002 (1993).
[32] A. J. Baltz, M. J. Rhoades-Brown, and J. Weneser, Phys. Rev. E **54**, 4233 (1996).
[33] A. J. Baltz, Phys. Rev. Lett. **78**, 1231 (1997).
[34] A. J. Baltz, M. J. Rhoades-Brown, and J. Weneser, Phys. Rev. A **44**, 5569 (1991).
[35] A. J. Baltz, M. J. Rhoades-Brown, and J. Weneser, Phys. Rev. A **47**, 3444 (1993).
[36] B. I. Abelev *et al.*, Phys. Rev. Lett. **102**, 112301 (2009).